



# Impact of Brine Discharge from Seawater Desalination Plants on Persian/Arabian Gulf Salinity

Hamed D. Ibrahim, Ph.D.<sup>1</sup>; and Elfatih A. B. Eltahir, Sc.D.<sup>2</sup>

**Abstract:** The Persian Gulf (also known as Arabian Gulf) is surrounded by desalination plants with about 50% of worldwide capacity to desalinate seawater. Most of these plants dispose of hypersaline effluent (brine) via surface and nearshore outfall into the Gulf. Because energy for desalination increases with seawater salinity, buildup of salt in brine endangers potable water supply there. Brine also contains metals and chemicals (foreign to the marine environment) that have adverse effects on marine ecosystems. Here, for the first time, brine is introduced into Gulf evaporation-driven residual circulation, which controls subbasin flushing, to quantify brine impact on salinity at basin and regional scales. Salt buildup increased mean annual basin salinity (40.5 g/kg) by only 0.43 g/kg, which confirms that basin salinity is insensitive to brine. But regional sensitivity to brine is significant, especially in the southwestern Gulf region near the Arabian coast, where the largest salt buildup raised salinity by about 4.3 g/kg. The results of this study suggests a significant role for brine outfall position in determining brine impact on regional salt levels. DOI: [10.1061/\(ASCE\)EE.1943-7870.0001604](https://doi.org/10.1061/(ASCE)EE.1943-7870.0001604). © 2019 American Society of Civil Engineers.

## Introduction

The purpose of this study is to offer a scientific basis for multinational efforts to ensure sustainable seawater desalination in the Persian/Arabian Gulf, hereafter Gulf. In Southwest Asia, where the climate is arid and precipitation is low, many population centers around the Gulf depend on potable water produced from desalinated seawater. The six-member countries of the Gulf Cooperation Council (GCC), Bahrain, Kuwait, Qatar, Saudi Arabia, United Arab Emirates (UAE), and Oman (Fig. 1), produce about 50% of worldwide desalinated seawater using intake seawater from the Gulf (Lattemann and Höpner 2008). The Gulf is also used for the disposal of brine, which contains, in addition to salt, pretreatment biocides (e.g., chlorine), coagulants (cationic and anionic polyelectrolytes), antiscalants (e.g., H<sub>2</sub>SO<sub>4</sub>), antifoaming agents, and heavy metals (e.g., copper) from plant corrosion (Alameddine and El-Fadel 2007; Hashim and Hajjaj 2005). Buildup of brine constituents endangers Gulf marine ecosystems (Sale et al. 2011; Dupavillon and Gillanders 2009; Roberts et al. 2010). Moreover, because energy for desalination increases with seawater salinity (Voutchkov 2018), salt buildup also threatens potable water supply for population centers around the Gulf.

Gulf evaporation by far exceeds freshwater input from river runoff and precipitation (Johns et al. 2003; Xue and Eltahir 2015). To balance this freshwater deficit, residual circulation brings Indian Ocean waters into the Gulf, while hypersaline water that contains all the salt left behind after evaporation flows back to the Indian

Ocean as part of this same circulation. It has long been known that the environmental impact of brine discharge into the Gulf, at all spatial scales, cannot be discussed separately without regard to Gulf residual circulation (Höpner and Windelberg 1997; Morton et al. 1997). Yet no impact study of brine discharge in the Gulf, at basin or regional scales, has been conducted that also considers Gulf residual circulation dynamics. Available impact studies, including brine discharge–tidal current interaction (Al-Barwani and Purnama 2008), near-field (short-term) impact of brine discharge from single plants (Altarayan and Madany 1992), and brine discharge along coastal sections (Purnalna et al. 2003) do not consider Gulf residual circulation dynamics.

In ocean effluent disposal via nearshore outfall, steady-state effluent concentration in areas significantly removed from outfall position depends on source strength and on spatiotemporal variations of ambient currents that flush the receiving water body (Camacho and Martin 2013; Roberts et al. 2011; Roberts 1999; Nakatsuji and Fujiwara 1997; Koh and Brooks 1975). Estimates of flushing currents, obtained in far-field analysis during offshore outfall design process, are vital to assessing the efficiency of effluent transport from the receiving water body to the open ocean (Blumberg et al. 1996; Guo and Lordi 2000). Moreover, in oceanic basins such as the Gulf where a basin-scale residual circulation controls subbasin flushing, it is necessary to evaluate the quiescent characteristics of this circulation as well as its modification after effluent discharge (Baum et al. 2018; Bleninger and Jirka 2008; Tsiourtis 2008; Palomar and Losada 2010; Malfeito et al. 2005).

Several authors have highlighted the complex and costly nature of far-field sampling of ocean currents and effluent concentrations, which is necessary to give a synoptic view of flushing in the receiving water body before and after effluent discharge (Bleninger and Jirka 2008; Roberts 1999). Roberts et al. (2011), in an observational study of Boston outfall, suggested that this difficulty of sampling may explain the scarcity of well-documented far-field studies of plume dispersion dynamics in the literature. Numerical models are a common and cheaper method of far-field analysis. Pérez-Díaz et al. (2019) recently showed that, even for oceanic basins with complex coastal topography, such as the Gulf, high-resolution three-dimensional (3D) hydrodynamic models with an unstructured

<sup>1</sup>Formerly, Ph.D. Candidate (Now Research Affiliate), Dept. of Civil and Environmental Engineering, Massachusetts Institute of Technology, Ralph M. Parsons Laboratory, Room 48–207, 77 Massachusetts Ave., Cambridge, MA 02139 (corresponding author). ORCID: <https://orcid.org/0000-0002-4720-3476>. Email: [hameddibrahim@gmail.com](mailto:hameddibrahim@gmail.com)

<sup>2</sup>Professor, Dept. of Civil and Environmental Engineering, Massachusetts Institute of Technology, Ralph M. Parsons Laboratory, Room 48–207, 77 Massachusetts Ave., Cambridge, MA 02139. Email: [eltahir@mit.edu](mailto:eltahir@mit.edu)

Note. This manuscript was submitted on May 18, 2018; approved on April 11, 2019; published online on September 28, 2019. Discussion period open until February 28, 2020; separate discussions must be submitted for individual papers. This paper is part of the *Journal of Environmental Engineering*, © ASCE, ISSN 0733-9372.

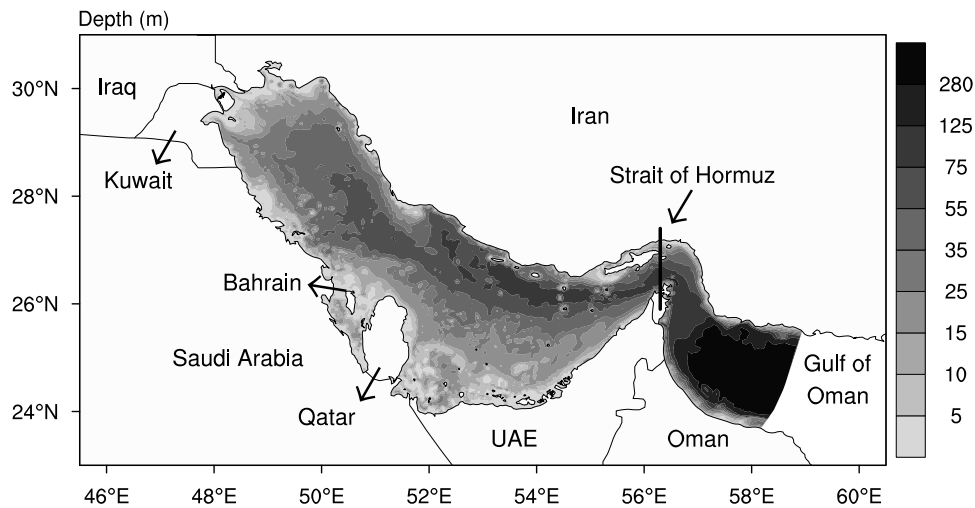


**Fig. 1.** Gulf depth profile; mean depth is approximately 35 m, and depth decreases from east to west. (Data from Amante and Eakins 2009.)

grid can simulate both near- and far-field brine dispersion dynamics in a consistent manner. Baum et al. (2018) concluded that computational fluid dynamics methods may be necessary to capture the dynamic interplay between brine discharge and ambient currents in the receiving environment.

Because salt can be considered a tracer, Gulf regions where brine discharge causes salt buildup indicate slow flushing zones. Xue and Eltahir (2015) used the high-resolution coupled Gulf-Atmosphere Regional Model (GARM), with a 3D unstructured grid hydrodynamic component, to estimate a Gulf basin flushing time of about 14 months. The novelty of this study is the simulation of the dynamic interplay between brine discharge and Gulf residual circulation, in order to quantify brine impact on Gulf basin and regional salinities. Three scenarios simulated in GARM are compared and analyzed: reference scenario (no brine discharge into Gulf residual circulation), 24-plant (largest plants in the Gulf) brine discharge scenario, and 14-plant (largest plants outside southwestern Gulf region) brine discharge scenario.

## Materials and Methods

### Model Description

Only a brief description of GARM, as related to simulation of Gulf residual circulation, is given here. However, a detailed description of GARM that includes sensitivity analysis can be found in Xue and Eltahir (2015), where GARM is used to estimate Gulf heat and water budgets. The atmospheric component of GARM is the Massachusetts Institute of Technology (MIT) Regional Climate Model (MRCM), an advanced version of Regional Climate Model version 3 that is maintained and distributed by the Abdus Salam International Center for Theoretical Physics, Trieste, Italy. MRCM has been used successfully to simulate regions with diverse climatic conditions (Im et al. 2014; Im and Eltahir 2018). The ocean component of GARM that simulates Gulf hydrodynamics is the Finite Volume Community Ocean Model (FVCOM) version 2.7. FVCOM is an unstructured grid, finite-volume, three-dimensional, primitive equation ocean model (Chen et al. 2003). Because its unstructured grid is ideal for complex topography, FVCOM is widely used for coastal and estuarine studies, as well as studies to assess flushing patterns in shallow oceanic regions (Kim et al. 2012; Rego et al. 2010). GARM includes the two-way interactions between MRCM and FVCOM with a coupling frequency of 3 h.

### Model Setup

Because of the different spatial scales of atmospheric and Gulf residual circulation, MRCM is configured to cover a larger domain between 29–61°E longitude and 12–40.5°N latitude with 30-km resolution in 120 × 120 grids. To simulate residual circulation characteristics in the Gulf, especially in the shallow regions near the Gulf Arabian coast where many seawater desalination plants withdraw seawater and discharge brine, GARM-FVCOM is configured with high horizontal resolution, which varies from 2 to 3 km near the coast, 5 km in offshore regions, and 10–15 km at the open ocean boundary. The Gulf is a shallow water system with a mean depth of approximately 35 m. Accordingly, in Gulf regions with water depths of less than 60 m, GARM-FVCOM is configured with 30 generalized sigma layers, whereas in Gulf regions with water depths greater than 60 m, the thickness of the top and bottom five layers is set to 2 m, and the other 20 intermediate layers are then uniformly divided for the remaining water column. This provides a vertical resolution of less than 1 m for nearshore Gulf regions and 1–2 m in most offshore Gulf regions. Gulf flushing time (to exchange all Gulf waters with Indian Ocean waters) is only about 14 months, and diurnal and seasonal cycles dominate Gulf variability (Xue and Eltahir 2015). Accordingly, the simulation period for all scenarios in this study is one decade (1981–1990), which is adequate to quantify the long-term dynamical interaction between brine discharge and Gulf residual circulation.

### Forcing and Initial Conditions

At the open ocean boundary, GARM-FVCOM uses climatological monthly mean fields of temperature (Locarnini et al. 2010) and salinity (Antonov et al. 2010), which consists of 1 degree objectively analyzed in situ temperature and salinity at standard depth levels. To resolve the wind-driven and buoyancy-driven mean flow components, GARM-FVCOM dynamically calculates mean flow velocity boundary conditions with wind, water temperature, and salinity information. River runoff into the Gulf from the Shatt Al Arab, the main source of freshwater to the Gulf, was specified based on streamflow statistics for the Tigris and Euphrates River basins (Saleh 2010). The reference and brine discharge scenarios were all initialized in GARM-FVCOM with the same (spatially variable) salinity and temperature values, which are based on available measurements taken in different Gulf areas.

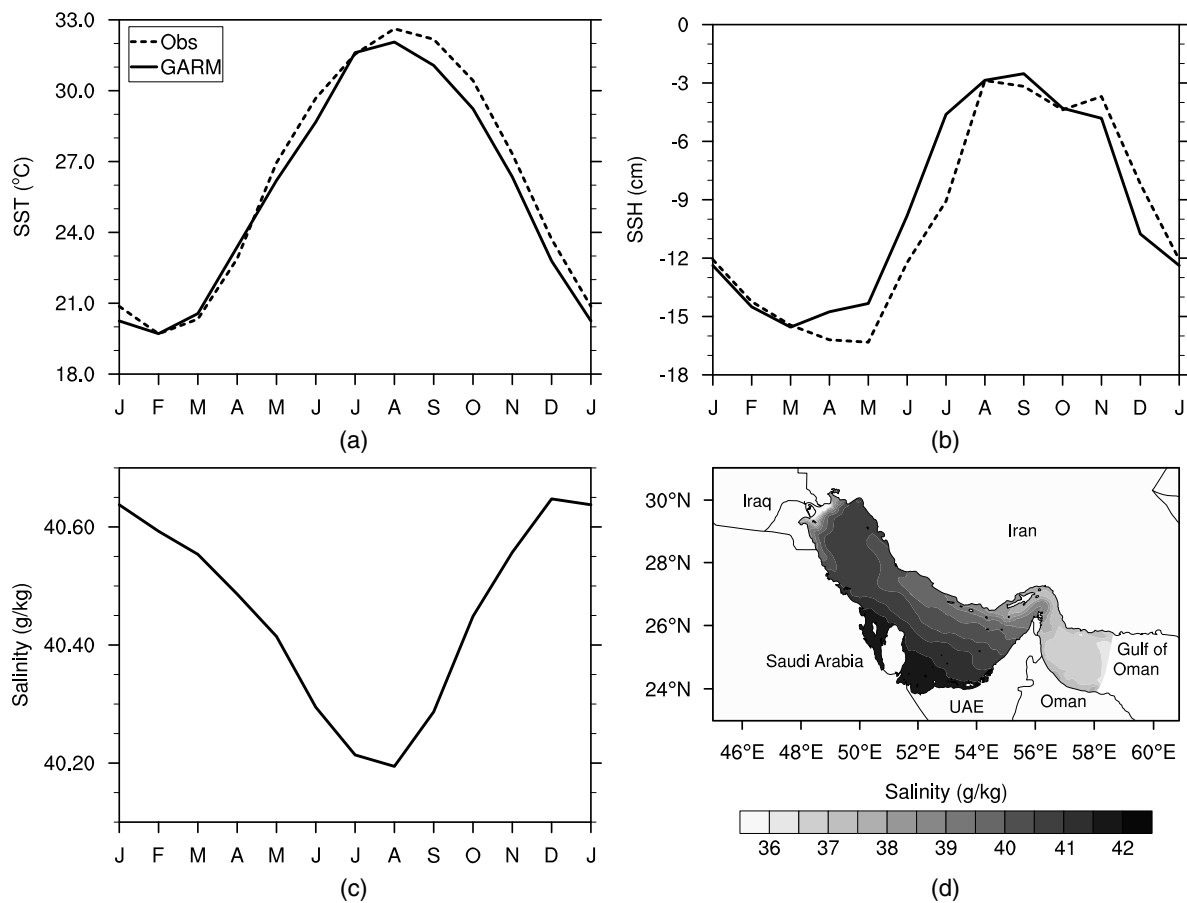


**Fig. 2.** Gulf residual circulation dynamic properties: (a) simulated versus analysis SST; (b) simulated versus satellite-derived Gulf sea surface height ( $SSH_G$ ); (c) simulated basin-average salinity; and (d) simulated basin-average salinity spatial distribution.

### Reference Scenario Simulation and Model Validation

Gulf seasonal water balance in Eq. (1), which includes the residual circulation exchange fluxes at the Strait of Hormuz between the Gulf and the Indian Ocean, is simulated in the reference scenario, hereafter Experiment 1 (Exp1). Introducing  $A_G$  ( $m^2$ ) for Gulf surface area (about 250,000  $km^2$ ), Gulf sea surface height monthly departure is given by

$$SSH_{G_t} = \frac{1}{A_G} \left\{ \oint P_t df + \oint E_t df + R_t + L_{IN_t} - L_{OUT_t} \right\} \quad (1)$$

where  $SSH_{G_t}$  (m) = Gulf basin-average sea surface height departure for month  $t = 1 \dots 12$ ;  $P$  (m);  $E$  (m) = monthly precipitation and evaporation respectively over and from an element  $df$  of the Gulf surface, where the integration is taken over the entire Gulf surface area;  $R$  ( $m^3$ ) = monthly volume of river runoff into Gulf;  $L_{IN}$  ( $m^3$ ) = monthly lateral volume flux into Gulf from Indian Ocean;  $L_{OUT}$  ( $m^3$ ) = monthly lateral volume flux out of Gulf to Indian Ocean; and  $L_{IN}$  and  $L_{OUT}$  = residual circulation exchange fluxes, and the monthly and annual characteristics of this exchange are detailed in Xue and Eltahir (2015). The focus in this study is on the residual circulation spatial variability within the Gulf.

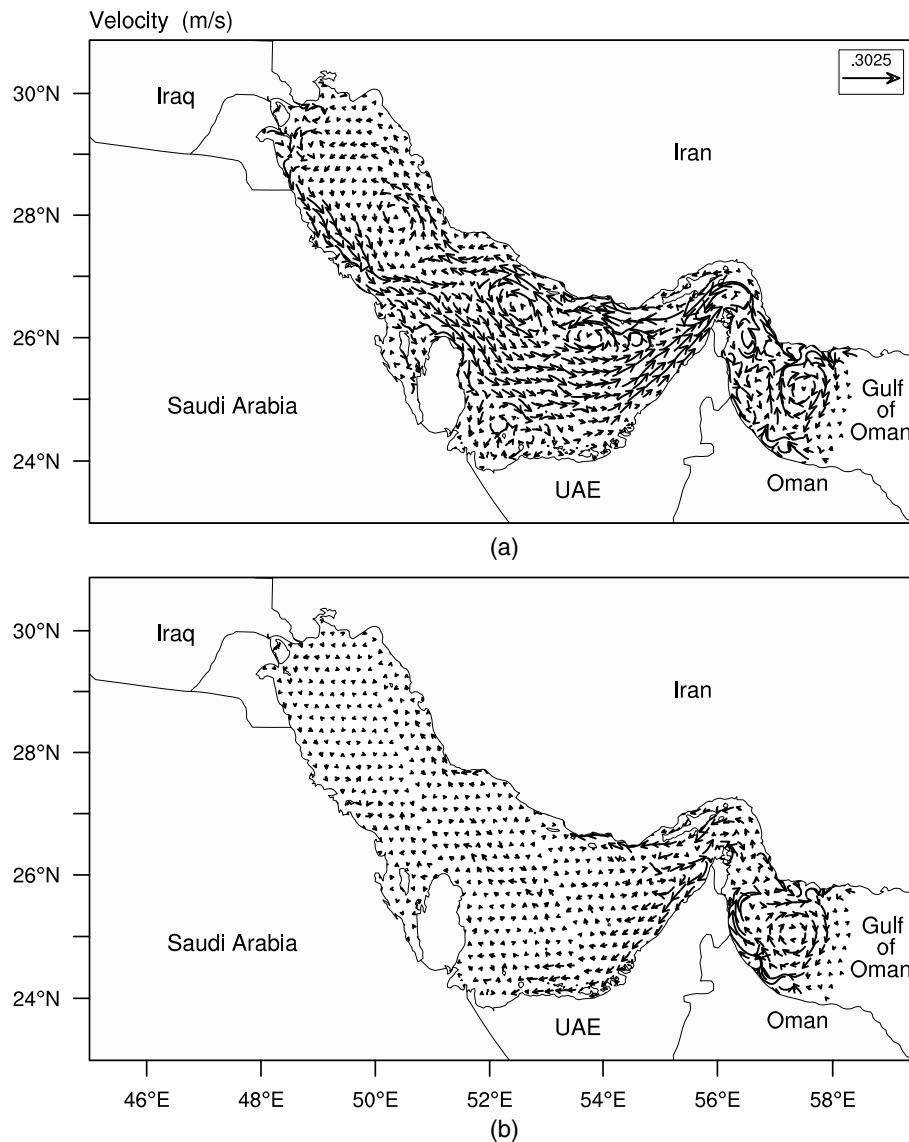
At the climatological monthly time scale (long-term monthly average), comparison of simulated Gulf sea surface height and temperature with satellite-derived Gulf sea surface height (Aviso 2017) and analysis temperature (Reynolds et al. 2007) shows that GARM simulates Gulf residual circulation with high accuracy

[Figs. 2(a and b)]. Simulated annual mean basin salinity is about 40.5 g/kg, which varies from a minimum in August to a maximum in January [Fig. 2(c)]. Because Tigris and Euphrates river runoff dilutes seawater in the northern regions, salinity there is the lowest in the Gulf [Fig. 2(d)]. Moreover, the salinity spatial distribution and Gulf water depth gradient are related [Figs. 1 and 2(d)]. Gulf regions near the northern Persian coast, where the Gulf is deep, have the smallest regional salinity, while the southwestern Gulf region near the Arabian coast, where the Gulf is shallow, has the largest regional salinity. Basin-scale observational studies of Gulf salinity are scarce, but comparison of recent near-surface salinity measurements around Kuwait Bay and offshore from UAE (Table 1) with simulated salinity shows that GARM correctly describes the spatial distribution of salinity in Gulf residual circulation.

Salinity spatial distribution is related to residual circulation horizontal velocity variation and lateral extent. In most Gulf regions, except the shallow southwestern Gulf region with the largest salinity [Fig. 2(d)], residual circulation horizontal velocity varies from a maximum in June to a minimum in November (Fig. 3). There are, however, other shallow coastal regions such as the northwestern and southeastern regions near the Arabian coast where regional salinity is less than southwestern regional salinity [Figs. 1 and 2(d)]. This suggests that nearshore flushing patterns within the Gulf depend on both coastal topography and the residual circulation currents. Accordingly, guided by this simulated salinity spatial distribution, two brine discharge scenarios were simulated in GARM and compared to Exp1 in order to quantify brine discharge

**Table 1.** Observed salinity near Arabian Gulf coast

Date	Longitude	Latitude	Salinity (g/kg) min–max	Source
November 13, 2014	53.2	24.25–24.75	40.02–42.99	Mezhoud et al. (2016)
July 7, 2013	53.6	24.2–24.75	41.30–4270	
June 6, 2013	54	24.2–24.25	42.00–44.7	Devlin et al. (2015)
October 8, 2013	54.4	24.25–25.4	39.38–43.00	
March 6, 2014	54.8	24.75–25.25	39.69–41.95	
2006–2013	47.7	29.24	48.0–48.7	
	48.07	29.19	34.2–45.6	
	48.2	29.06	34.3–45.3	
	48.25	28.43	36.1–43.9	

**Fig. 3.** Gulf residual circulation (RS) horizontal velocity spatial variation: (a) depth-averaged maximum RS horizontal velocity when lateral extent of RS is at maximum (June); and (b) depth-averaged minimum RS horizontal velocity when lateral extent of RS is at minimum (November).

impact on salinity at basin and regional scales and assess flushing patterns in Gulf nearshore regions.

### Method of Simulating Brine Discharge

In seawater desalination the primary objective is to produce potable water by removing salt from seawater. For a given potable

water production capacity  $V_p$  ( $m^3$ ), the interaction of a seawater desalination plant with an oceanic basin involves intake of a given volume of seawater  $V_I$  ( $m^3$ ) (often two to three times  $V_p$ ) of salinity  $S_I$  (g/kg) and discharge of brine (approximately equal to  $V_p$  and having a salinity of up to twice  $S_I$ ) into the basin (Morton et al. 1997; Einav and Lokiec 2003). Introducing  $V_D$  ( $m^3$ ) for brine volume discharge into the sea and  $\rho$  ( $kg/m^3$ ) for density,



**Table 2.** Largest (capacity  $\geq 100,000$  m<sup>3</sup>/day) 24 seawater desalination plants in Gulf

Plant ID	Country	Capacity (m <sup>3</sup> /day)	Status
1	Bahrain	272,760	O
2	Bahrain	218,000	O
3	Bahrain	136,380	O
4	Kuwait	622,400	O + C
5	Kuwait	454,600	O
6	Kuwait	227,300	C
7	Kuwait	204,390	O
8	Kuwait	136,260	O
9	Kuwait	261,840	O
10	Qatar	741,160	O
11	Qatar	545,250	C
12	Qatar	654,606	O
13	Saudi Arabia	1,011,814	O + C
14	Saudi Arabia	1,025,000	O + C
15	Saudi Arabia	432,580	O
16	UAE	636,440	O
17	UAE	913,346	O
18	UAE	874,460	O
19	UAE	1,226,950	O
20	UAE	503,061	O
21	UAE	306,500	O
22	UAE	140,000	C
23	UAE	102,144	O
24	UAE	100,000	C

Note: O = plant is online; C = plant is under construction; and O + C = plant is being expanded; and UAE = United Arab Emirates.

mass conservation of salt and water in the desalination processes is given by

$$\rho_I V_I S_I = \rho_D V_D S_D \quad (2)$$

$$\rho_D V_D = \rho_I V_I - \rho_P V_P \quad (3)$$

Assuming negligible salt content in the potable water produced, from Eq. (2) the mass of salt in brine discharge is equal to the mass of salt in intake seawater. However, from Eq. (3) the mass of water in brine discharge is the difference of the mass of water in intake seawater and the mass of produced potable water. Therefore, seawater desalination can be described as a freshwater sink in an oceanic basin. Various methods are used to desalinate seawater, including electrodialysis, electrodialysis reversal, reverse osmosis, multistage flash distillation, multieffect distillation, and vapor compression distillation. These methods often have different ratios of seawater intake to brine discharge capacity. However, in this study, seawater desalination plants' brine discharges are simulated in GARM as freshwater sinks.

There are more than 850 seawater desalination plants in the Gulf. Most of these plants, including the 24 largest (based on production capacity  $\geq 100,000$  (m<sup>3</sup>/day), are located on the Arabian coast near the shallow ( $\leq 15$  m) southwestern region of the Gulf (Global Water Intelligence 2016). For practical reasons, and since small plants are assumed to have negligible impacts, only brine discharge from the 24 largest plants are considered in this study (Table 2). Based on available design parameters for existing seawater desalination plants in the Gulf, brine discharge points for all plants in the brine discharge scenarios are placed at about 2 km offshore.

### Design of Brine Discharge Scenarios

Two brine discharge scenarios were simulated in GARM (Table 3). Brine from the 24 largest plants in the Gulf [Fig. 4(a)] is introduced

**Table 3.** Brine discharge configurations for all scenarios

Scenario ID	Brine discharge	Plant ID
Exp1	No	—
Exp2	Yes	1–24
Exp3	Yes	4–9, 13–14, 16, 18–21, 24

Note: Brine discharge from Plants 1–3, 10–12, 15, 17, 22, and 23 are excluded from Exp3.

into Gulf residual circulation dynamics in the first brine discharge scenario, hereafter Experiment 2 (Exp2), and Exp2 is compared to Exp1 (reference scenario) to quantify the brine discharge impact on Gulf salinity at basin and regional scales. In the second brine discharge scenario, hereafter Experiment 3 (Exp3), brine discharge from the 10 plants within the southwestern Gulf region are excluded from Gulf residual circulation dynamics, and only brine from the 14 plants outside this region are introduced into the residual circulation [Fig. 4(b)]. Accordingly, the relative impact of brine discharge within and outside the shallow southwestern Gulf region (Fig. 5), where regional salinity is greatest [Fig. 2(d)], is obtained by comparing Exp3 with Exp2. Because Gulf residual circulation does not vary annually within the southwestern region (Fig. 3), comparison of Exp3 with Exp2 also shows the effect of coastal topography on flushing patterns in this region.

### Methods of Brine Discharge Impact Analysis

Salinity can be considered as a conservative tracer that describes the dynamical interaction between brine discharge and Gulf residual circulation. Accordingly, to characterize this dynamical interaction, model-predicted results for Exp1, Exp2, and Exp3 are compared by analyzing monthly time series of area-averaged salinity for three Gulf areas. The first area is the whole Gulf basin up to the Strait of Hormuz, hereafter referred to as the basin. The second area has the largest salinity in the Gulf's southwestern region, the region between the coasts of Saudi Arabia, Bahrain and Qatar (henceforth Reg1). The third area is the Gulf region 20 km off the Arabian coast where the 24 largest seawater desalination plants in the Gulf discharge brine (henceforth Reg2). Because the only factor that differentiates Exp1, Exp2, and Exp3 is brine discharge into the Gulf's residual circulation dynamics, a one-way analysis of variance (ANOVA) is performed to compare brine discharge impact on area-average salinity in Exp1, Exp2, and Exp3 for each of the three areas chosen for impact analysis. Thus, the ANOVA statistical analysis tests the null hypotheses given in Eqs. (4)–(6):

$$H_{0,\text{basin}}: \mu_1 = \mu_2 = \mu_3 \quad (4)$$

$$H_{0,\text{Reg1}}: \mu_1 = \mu_2 = \mu_3 \quad (5)$$

$$H_{0,\text{Reg2}}: \mu_1 = \mu_2 = \mu_3 \quad (6)$$

where  $\mu$  = area-average salinity in Exp1, Exp2, and Exp3 for the three areas, respectively.

## Results

### Basin-Scale Brine Discharge Impact

Comparison of Exp1 and Exp2 basin-average salinity shows that brine discharge into the Gulf caused salt buildup that increased basin salinity by 0.43 g/kg [Figs. 6(a and b)]. This basin salt buildup is not spatially uniform. In the Gulf's northern and northwestern

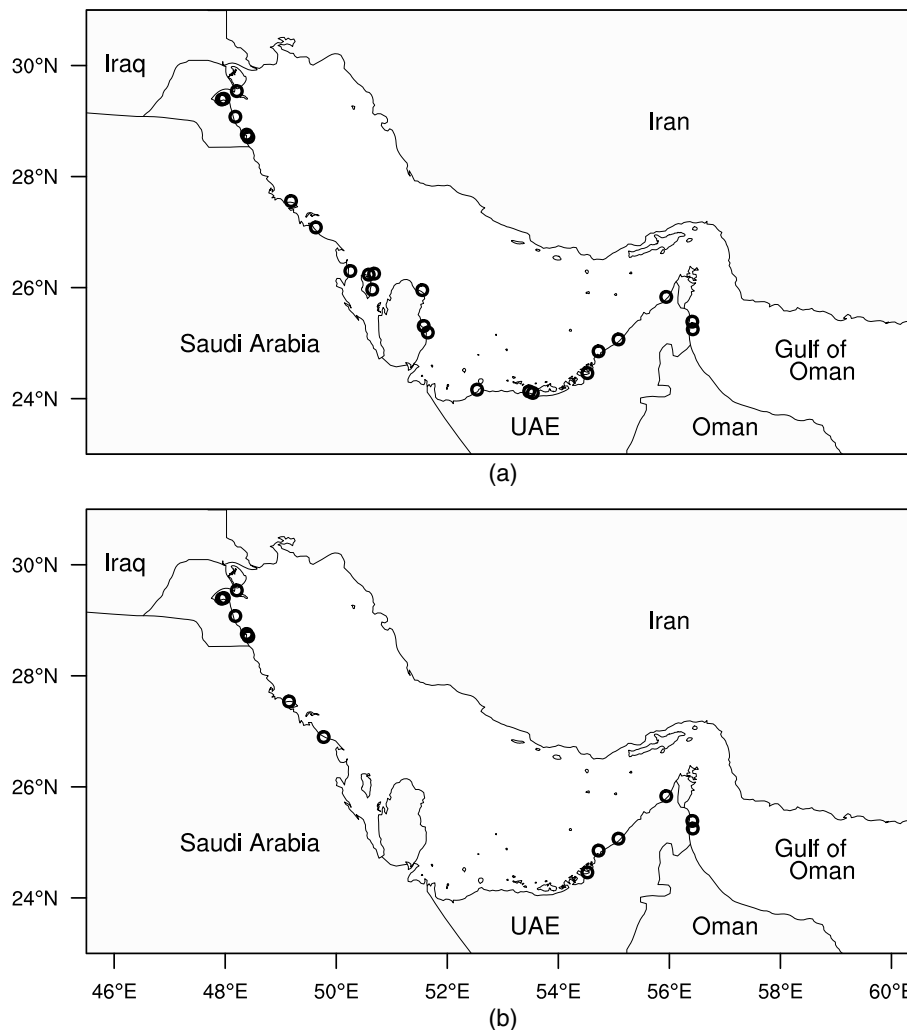


**Fig. 4.** Design of brine discharge scenarios: (a) location of 24 largest seawater desalination plants simulated in Exp2; and (b) location of 14 largest plants outside southwestern Gulf region simulated in Exp3. Discharge position for all plants in Exp2 and Exp3 are approximately 2 km offshore.

regions, salt buildup is small and change in salinity (Exp2 minus Exp1) is in the range of 0–1 g/kg. However, there is considerable salt buildup in the Gulf's southern and southwestern regions near the Arabian coast [Fig. 6(a)], especially between Saudi Arabia, Bahrain, and Qatar, where the change in salinity reaches up to 7 g/kg. Furthermore, because of brine discharge, the difference between annual maximum and minimum Gulf basin-average salinity (salinity seasonal cycle amplitude) also increased from about 0.6 g/kg in Exp1 to 1 g/kg in Exp2 [Fig. 6(b)].

### Regional-Scale Brine Discharge Impact

In Reg1, where Plants 1–3 and 15 discharge brine [Fig. 6(c)], salinity (the largest in the Gulf) increased by about 4.3 g/kg because of salt buildup [Fig. 6(d)]. In Reg2, the area up to 20 km offshore from the Gulf's Arabian coast where the largest seawater desalination plants in the Gulf discharge brine [Fig. 6(e)], salt buildup because of brine discharge raised salinity by 1.6 g/kg [Fig. 6(f)]. However, most of the salt buildup that raised Reg2 salinity occurred in the Gulf's southwestern region near the Arabian Coast, especially the salt buildup in Reg1 [Fig. 6(a)].

Brine discharge into the Gulf's residual circulation dynamics changed the temporal characteristics of salt buildup within the Gulf.

In the first year of Exp1, Reg1 salinity increased to a maximum of about 42 g/kg and remained at this value without seasonal variation for the rest of the Exp1 simulation [Fig. 6(d)]. There is, however, seasonal variation in Reg1 salinity after the first year of Exp2 [Fig. 6(d)]. In the first year of Exp2, Reg1 salinity increased rapidly to reach about 45 g/kg; for the next 5 years the salinity increased slowly to a maximum of approximately 46.5 g/kg and remained at this value for the rest of the Exp2 simulation [Fig. 6(d)]. Like Reg1, Reg2 salinity also increased rapidly in Exp2 [Fig. 6(f)], but in both Exp1 and Exp2 there is seasonal variation in Reg2 salinity.

### Relative Impact of Brine Discharge within and outside Southwestern Gulf Region

When brine is not discharged into the Gulf's southwestern region, the Exp3 simulation, salt buildup in the Gulf decreased [Fig. 7(a)]. Compared to the increase in basin salinity in Exp2 (0.45 g/kg), basin salinity increased by only 0.2 g/kg in Exp3 [Fig. 7(b)]. Salt buildup in Reg1 and Reg2 decreased from 4.3 and 1.6 g/kg in Exp2 to 0.8 and 0.6 g/kg, respectively, in Exp3 [Figs. 7(c–f)]. The temporal characteristics of salt buildup also changed in Exp3. During the first year of Exp3, Reg1 salinity increased to a first maximum of approximately 42 g/kg and remained at this

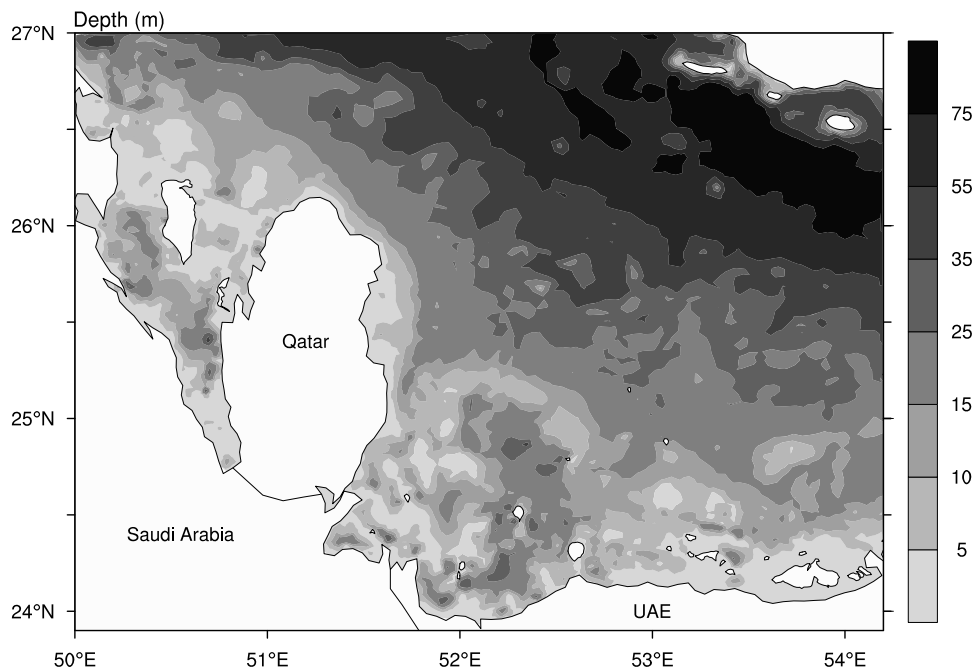


Fig. 5. Southwestern Gulf region with largest regional salinity.

value for another 4 years; then the salinity increased again to a second maximum of approximately 42.5 g/kg and remained at this value for the rest of Exp3 [Fig. 7(d)]. As in Exp1, Reg1 salinity does not have significant seasonal variation in Exp3. The Reg2 salinity seasonal cycle amplitude, however, is larger in Exp3 compared to Exp1 and smaller in Exp3 compared to Exp2 [Fig. 7(f)].

## Discussion

### Resilience of Gulf Basin Salinity to Brine Discharge

As expected, with a basin salinity increase of only about 0.43 g/kg in Exp2 compared to Exp1, brine discharge (seawater desalination freshwater sink) only had a slight impact on Gulf basin salinity. This is because the Gulf freshwater sink due to seawater desalination—about 5 km<sup>3</sup>/year—is by far smaller than the Gulf freshwater sink due to evaporation—about 390 km<sup>3</sup>/year; consequently, brine discharge does not significantly affect Gulf flushing time by the evaporation-driven residual circulation between the Gulf and the Indian Ocean (Ibrahim 2017). This circulation, which inhibits basin salt buildup, has the character of an antiestuarine circulation (Thoppil and Hogan 2010; Sadrasab and Kämpf 2004; Reynolds 1993; Sugden 1963), and Gulf sea surface height ( $SSH_G$ ) controls surface lateral inflow ( $L_{IN}$ ) from the Indian Ocean to the Gulf.  $L_{IN}$  is large when  $SSH_G$  is low, relative to the Indian Ocean, whereas  $L_{IN}$  is small when  $SSH_G$  is high, relative to the Indian Ocean. Bottom lateral outflow from the Gulf to the Indian Ocean ( $L_{OUT}$ ) is controlled by the pressure difference between Gulf waters and Indian Ocean waters: thus,  $L_{OUT}$  is large when the pressure acting on Gulf bottom waters is high, relative to Indian Ocean waters at the same depth, and vice versa. Thus, when  $SSH_G$  decreases because of freshwater removal, as in evaporation or seawater desalination,  $L_{IN}$  increases. Because the additional water and salt in  $L_{IN}$  increases the weight acting on Gulf bottom waters, relative to the Indian Ocean,  $L_{OUT}$  also increases accordingly, and basin salt buildup is inhibited (Ibrahim 2017). Compared to evaporation that changes  $SSH_G$  by about 1.56 m/year, seawater

desalination changes  $SSH_G$  by about 0.02 m/year. Accordingly, brine discharge is unlikely to significantly change the period for Gulf flushing by the residual circulation, as demonstrated by the small difference between Exp1 and Exp2 basin salinity seasonal cycle amplitude [Fig. 6(b)].

There are, however, large differences in regional salt buildup within the Gulf after brine discharge [Figs. 6(a) and 7(a)]. This indicates that the regional-scale dynamics of the residual circulation is more sensitive to brine discharge than the basin-scale dynamics of the residual circulation. Thus, regional flushing patterns reflect the residual circulation spatial variability within the Gulf.

### Gulf Residual Circulation Spatial Variability

Comparison of the spatial distribution of salinity in Exp1 with Exp2 and Exp3 yields considerable insight into the Gulf residual circulation–brine discharge interaction, as well as the spatial variability of this interaction. One-way ANOVA rejects the null hypothesis in Eq. (4) for the Gulf basin: the brine discharge impact on basin-average salinity was significant,  $F(2,357) = 88.35$ ,  $p = 0.000$ . Basin salinity in Exp2 and Exp3 after brine discharge is only slightly different from basin salinity in Exp1 [Fig. 7(b)], whereas the large regional salt buildup in Exp2 and Exp3 [Figs. 6(a) and 7(a)], especially in the Gulf's southwestern region, demonstrates that brine discharge significantly modified brine transport characteristics within the Gulf. Consequently, even though ANOVA shows basin salinity sensitivity to brine discharge (Table 4), the magnitude of this sensitivity in different Gulf regions depends on the local strength of Gulf residual circulation flushing.

The Gulf can be divided into two flushing zones that mostly correspond to the two regions where the residual circulation horizontal velocity is strong and weak [Fig. 3(a)]: (1) the fast flushing zone, which includes the northern and northwestern Gulf regions, and (2) the slow flushing zone, which includes the southern and southwestern Gulf region [Figs. 6(a) and 7(a)]. Consistent with the findings of Jiang et al. (2017) for a semienclosed bay in Southern China, comparison of Exp2 and Exp3 shows that basin

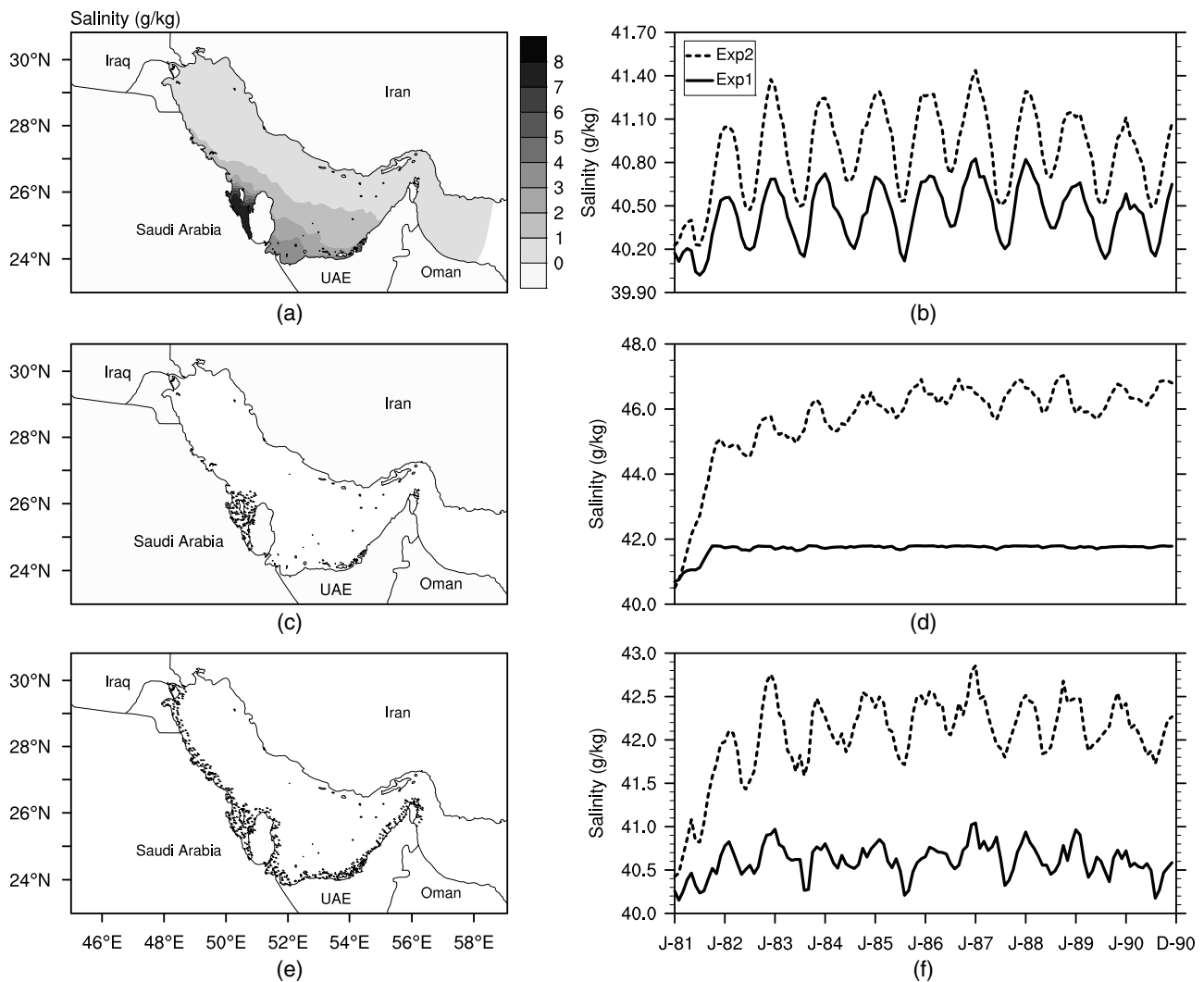


**Fig. 6.** Gulf salt buildup because of brine discharge: (a) average (depth and time) change in basin salinity (Exp2 minus Exp1); (b) monthly basin salinity; (c) Reg1: Southwestern Gulf region with largest regional salinity (hatched); (d) monthly Reg1 salinity; (e) Reg2: Gulf region 20 km offshore from Arabian coast (hatched); and (f) monthly Reg2 salinity.

salt buildup is minimized when brine is discharged into the Gulf's fast flushing zone instead of the slow flushing zone.

Regulatory conditions for outfall design often assume worst-case effluent concentration levels based on quiescent hydrodynamic conditions, which Roberts (1999) suggests might lead to overly conservative outfall designs. But Baum et al. (2018) found in an observational study that ambient salinity levels after brine discharge differed significantly from those assumed for outfall design. Because of the perception that background current conditions in the receiving environment aid effluent dispersion, the authors conclude, the effects of the dynamic interplay between ambient hydrodynamic conditions and brine discharge are often neglected in simple empirical models used for outfall design purposes. To improve brine dispersion, Bleninger and Jirka (2008) emphasized an iterative approach to outfall design, whereby sampling of salinity levels, after brine discharge, is used to modify outfall position. As demonstrated in Exp3, where salt buildup occurred in Gulf regions without brine discharge [Fig. 7(a)], the Gulf residual circulation–brine interaction is strong. Hence, the results here highlight the importance of the iterative approach to outfall design in the Gulf's slow flushing zones.

Because of the dynamic interplay between brine discharge and Gulf residual circulation, brine discharge has a remote impact in places far from the brine outfall position. Exp3 shows that even when brine is discharged only into fast flushing zones, because of this interplay, there is still salt buildup in Gulf slow flushing zones [Fig. 7(a)]. An important brine outfall design objective is to avoid recirculation of brine into intake seawater, which compromises plant operation efficiency. To satisfy this objective, feasibility studies in the Gulf often seek design criteria for sufficient physical separation between intake seawater and brine outfall position (Ng et al. 2001). Such design criteria, however, may be inadequate to prevent salt buildup without accounting for the brine discharge–residual circulation interaction, which promotes salt buildup in the Gulf's slow flushing zones even when brine is not discharged there.

### Regional Salt Buildup

The largest seawater desalination plants in the Gulf obtain seawater and discharge brine in nearshore regions (Reg2) of the shallow Gulf Arabian coast [Figs. 4(a) and 6(e)], and buildup of salt in



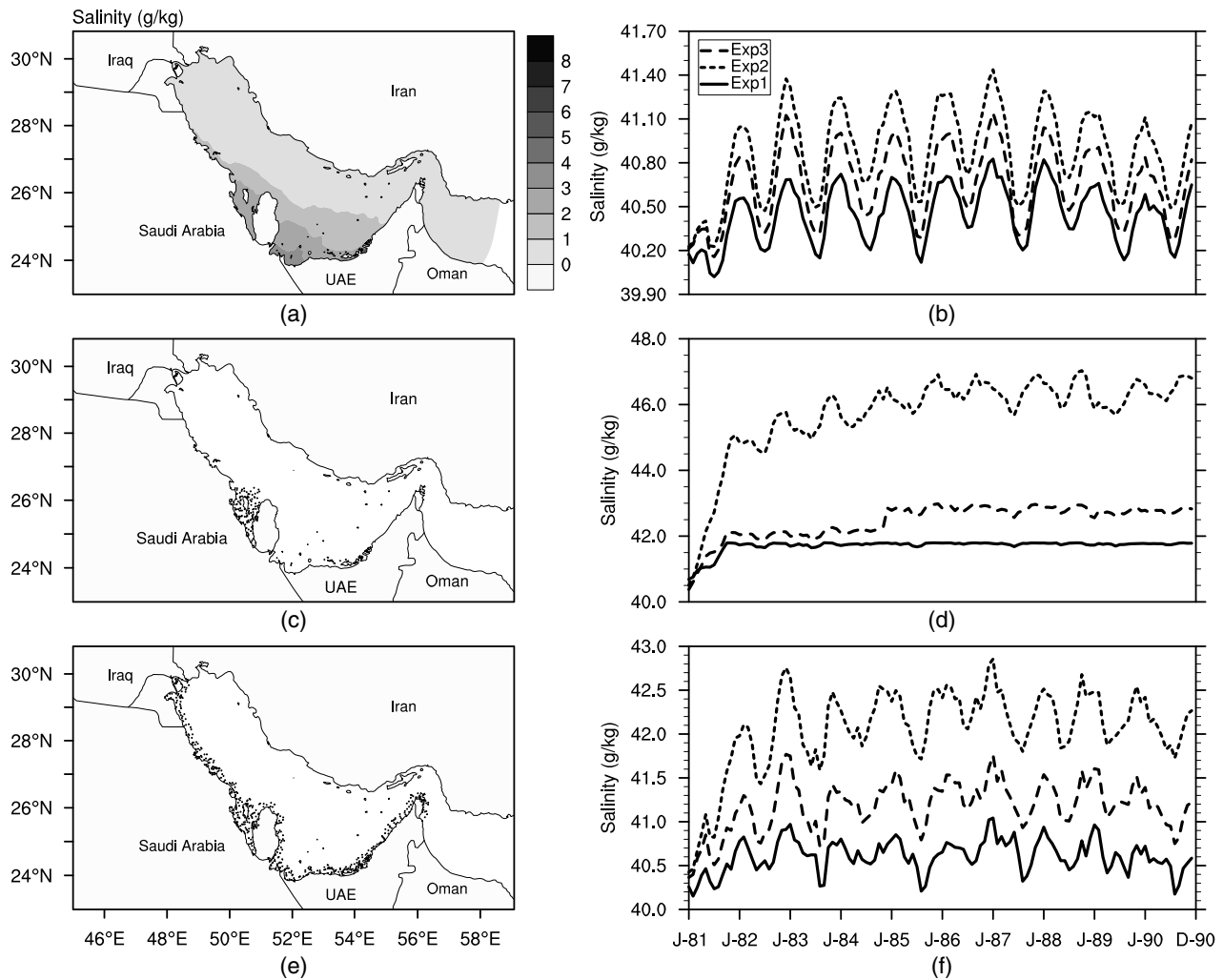


**Fig. 7.** Relative impact of brine discharge within and outside southwestern Gulf region: (a) average (depth and time) change in basin salinity (Exp3 minus Exp1); (b) monthly basin salinity; (c) Reg1: southwestern Gulf region with largest regional salinity (hatched); (d) monthly Reg1 salinity; (e) Reg2: Gulf region 20 km offshore from Arabian coast (hatched); and (f) monthly Reg2 salinity.

**Table 4.** ANOVA pairwise summary: impact of brine discharge on basin-average salinity

Scenarios	Mean difference	95% confidence interval		P-value
		Lower bound	Upper bound	
Exp1 Exp2	-0.4340	-0.5105	-0.3574	0.0000
Exp1 Exp3	-0.2101	-0.2866	-0.1335	0.0000
Exp2 Exp3	0.2239	0.1474	0.3004	0.0000

brine is largest on this coast, especially the southwestern region [Figs. 6(a) and 7(a)]. One-way ANOVA rejects the null hypothesis in Eqs. (5) and (6) for Reg1 and Reg2, respectively: the brine discharge impact on area-average salinity was significant in Reg1,  $F(2,357) = 886.36$ ,  $p = 0.000$ , and in Reg2,  $F(2,357) = 577.87$ ,  $p = 0.000$ . Area-average salinity in Reg1 and Reg2, which reflects the residual circulation flushing strength in these regions, is sensitive to brine discharge (Tables 5 and 6). Evidently, because flushing by residual circulation inhibits salt buildup at the basin scale, there must be upper limits to salt buildup in Reg1 and Reg2. These limits, moreover, will reflect local conditions in Reg1 and Reg2 that

**Table 5.** ANOVA pairwise summary: impact of brine discharge on Reg1 area-average salinity

Scenarios	Mean difference	95% confidence interval		P-value
		Lower bound	Upper bound	
Exp1 Exp2	-4.0273	-4.2658	-3.7888	0.0000
Exp1 Exp3	-0.7466	-0.9851	-0.5080	0.0000
Exp2 Exp3	3.2808	3.0422	3.5193	0.0000

modify the temporal and spatial characteristics of the residual circulation [Figs. 7(d) and (f)].

Comparison of Exp2 and Exp3 showed that salt buildup because of brine from the 14 plants with outfalls outside the Gulf's southwestern region, which collectively produce about 65% of the potable water capacity of all 24 plants ( $4.3 \text{ km}^3/\text{year}$ ), caused 35% of the increase in the southwestern region's salinity. However, salt buildup because of brine from the 10 plants with outfalls within the southwestern region, which collectively produce about 35% of the potable water capacity of all 24 plants, caused 65% of the increase in the southwestern region's salinity. This establishes the

**Table 6.** ANOVA pairwise summary: impact of brine discharge on Reg2 area-average salinity

Scenarios	Mean difference	95% confidence interval		P-value
		Lower bound	Upper bound	
Exp1 Exp2	-1.4560	-1.5571	-1.3549	0.0000
Exp1 Exp3	-0.5745	-0.6756	-0.4734	0.0000
Exp2 Exp3	0.8815	0.7804	0.9826	0.0000

Gulf's southwestern region as the most sensitive region to brine discharge where salt, as well as metals and reactive byproducts in brine, is likely to buildup.

### **Salt Trapping in Southwestern Gulf Region**

One possible explanation for salt trapping in the Gulf's southwestern region is the bathymetry of this region. There are many depressions in this region between Bahrain and the coast of Saudi Arabia and between the Coasts of Qatar and UAE, where water that is up to 25 m deep is surrounded by water that is only about 5–10 m deep (Fig. 5). These depressions will promote brine trapping. Because salt increases the weight of water, and heavy water sinks, salt will continue to build up in these depressions until the water column becomes stable. Furthermore, these deep depressions are separated from the east-bound flushing currents of the Gulf's residual circulation by shallow waters that act like a sill and inhibit dynamic interplay between brine discharge into the Gulf's southwestern region and the residual circulation [Figs. 3(a) and 5]. Accordingly, the southwestern region's bathymetry constrains the interactions with the Gulf's residual circulation: this limits the capacity of the circulation to flush this region and promotes salt buildup there up to a limit after which local factors that drive coastal currents, such as wind and tide, enhance the residual circulation flushing.

In a numerical study of Venice Lagoon, Cucco and Umgiesser (2015) showed that subbasin trapping, because of local conditions that affect basin-scale circulation, can yield regional flushing times that are significantly larger than the basin integral flushing time. A literature survey yielded no systematic study of brine trapping in nearshore regions on the Arabian Gulf coast. This is probably because of the relatively recent rapid expansion of seawater desalination in the Gulf. Pollutant trapping and flushing dynamics of trapped salt in other coastal settings have been reported. Debler and Imberger (1996) investigated the conditions necessary for river flow to completely flush a depression in an estuary that is filled with saline water. The authors found that if the speed of flow over the depression is fast, because this speed controls turbulent erosion of the density interface, it is possible to completely flush depressions filled with saline water. This finding was also confirmed in a numerical study by Zhang et al. (2008), where the effects of flow speed, and the depression slope on trapped saline water was evaluated. There is no river discharge into the nearshore southwestern Gulf region, and precipitation there is negligible (Ibrahim 2017). Accordingly, the tide is the only source of water for flushing trapped brine. However, Azam et al. (2006) showed that in the rocky southern Gulf, characterized by bathymetric undulations, tidal contributions to coastal currents are small, but wind-induced currents are strong. Because the Gulf's residual circulation inhibits basin salt buildup, this circulation also imposes upper limits on subbasin salt buildup. The estimates of these limits as given in this study [Figs. 6(a) and 7(a)] are a first step toward systematic characterization of brine trapping in slow flushing zones near Arabian Gulf coast.

## **Practical Applications and Future Research Perspectives**

### **Designing Brine Outfalls in Southwestern Gulf Region**

The freshwater that is removed from the Gulf by seawater desalination is only about 1.2% of Gulf basin evaporation (Ibrahim 2017), which drives the residual circulation that flushes the Gulf. Considerable benefit can be derived by taking advantage of the residual circulation flushing characteristics to enhance brine transport from the Gulf to the open ocean, especially in slow flushing zones such as the southwestern Gulf region. The findings here demonstrate the far-field dynamical interplay between the Gulf's residual circulation and brine discharge. A future research direction will be a systematic study, documented in a design manual, of outfall alternatives for slow flushing Gulf zones, whereby brine produced by plants near these zones is discharged into fast flushing zones where the residual circulation flushing is effective.

The far-field analysis given here for brine discharge on the Arabian coast, however, can be used to guide the design of brine outfalls near this coast, especially in the Gulf's southwestern region that is most sensitive to salt buildup. Although construction and maintenance costs of ocean outfalls increase exponentially with outfall length, long brine outfalls are sometimes necessary to avoid costly environmental damage to coastal marine ecosystems (Shahvari and Yoon 2014). One practical application of this study is to use the spatial and temporal characteristics of salt buildup because of brine discharge that is given here to evaluate alternative brine outfall positions in the southwestern Gulf region, so that brine is placed where residual Gulf circulation flushing is effective. A study that implements this approach will be presented in a separate paper.

### **Evaluating Harmful Algal Bloom Population Dynamics**

The small reduction in Gulf flushing time because of brine discharge may have increased the frequency of harmful algal blooms (HABs) in the Gulf. This is because the transport of formed HABs from the Indian Ocean to the Gulf is an important factor in Gulf HAB events, which has increased in recent decades (Shehhi et al. 2014). HABs (or red tide) have contributed to the death of large quantities of marine life in the Gulf (Al-Yamani et al. 2012; Sale et al. 2011; Glibert et al. 2002). HABs also foul intake seawater for desalination plants, which causes acute reductions in plant production capacity, plant shutdowns, and damage to membranes and other sensitive desalination equipment (Ghanea et al. 2016; Thu et al. 2014; Shehhi et al. 2014; Zhao and Ghedira 2014). Moreover, brine has also been identified as a source of inorganic nutrients for harmful algae (Roberts et al. 2010). This study provides spatial and temporal characteristics of salinity that can be used to identify and monitor Gulf regions at high risk of HABs because of brine discharge.

## **Conclusion**

For the first time, the dynamic interaction between brine discharge and the Gulf's residual circulation was simulated, and brine discharge impact was quantified at basin and regional scales. Because of this circulation, basin-scale salinity is resilient to brine discharge. However, regional sensitivity to brine discharge is large in the Gulf's southwestern region, and preventing salt buildup there may require multinational efforts. Jong (1989) observed that "the treaty establishing the GCC contains the enabling clauses to create a viable mechanism for implementing coordinated utilization of the

GCC's shared water resources within the accepted framework of international law." This study provides the scientific basis for coordinated utilization of Gulf seawater for desalination.

## Data Availability Statement

Some or all data, models, or code used during the study were provided by a third party.

- Gulf-Atmosphere Regional Model (GARM).

Direct requests for these materials may be made to the provider as indicated in the acknowledgments.

## Acknowledgments

Thank you to Dr. Pengfei Xue for providing the numerical model (GARM) used for this study (Xue and Eltahir 2015). Also, thank you to Dr. Yunfang Sun for invaluable technical assistance and constructive discussions during model setup. This work was achieved in partial fulfillment of the requirements for H. I.'s Ph.D. degree in Civil and Environmental Engineering (hydrology), defended on August 7, 2017, at MIT. Partial funding was provided by the Center for Complex Engineering Systems (CCES) at MIT and King Abdulaziz City for Science and Technology (KACST).

## References

- Alameddine, I., and M. El-Fadel. 2007. "Brine discharge from desalination plants: a modeling approach to an optimized outfall design." *Desalination* 214 (1–3): 241–260. <https://doi.org/10.1016/j.desal.2006.02.103>.
- Al-Barwani, H., and A. Purnama. 2008. "Simulating brine plumes discharged into the seawaters." *Desalination* 221 (1–3): 608–613. <https://doi.org/10.1016/j.desal.2007.02.060>.
- Altayaran, A., and I. Madany. 1992. "Impact of a desalination plant on the physical and chemical properties of seawater, Bahrain." *Water Res.* 26 (4): 435–441. [https://doi.org/10.1016/0043-1354\(92\)90043-4](https://doi.org/10.1016/0043-1354(92)90043-4).
- Al-Yamani, F., M. Saburova, and I. Polikarpov. 2012. "A preliminary assessment of harmful algal blooms in Kuwait's marine environment." Supplement, *Aquat. Ecosyst. Health Manage.* 15 (S1): 64–72. <https://doi.org/10.1080/14634988.2012.679450>.
- Amante, C., and B. W. Eakins. 2009. "ETOPO1 1 Arc-minute global relief model: Procedures, data source and analysis." Accessed October 9, 2015. <https://www.ngdc.noaa.gov/mgg/global/relief/ETOPO1/data/>.
- Antonov, J. I., D. Seidov, T. P. Boyer, R. A. Locarnini, A. V. Mishonov, H. E. Garcia, O. K. Baranova, M. M. Zweng, and D. R. Johnson. 2010. *World ocean atlas 2009, volume 2: Salinity*, 184. Edited by S. Levitus. Washington, DC: US Government Printing Office.
- Aviso. 2017. "Altimetry." Accessed June 15, 2015. [www.aviso.altimetry.fr/duacs/](http://www.aviso.altimetry.fr/duacs/).
- Azam, M. H., W. Elshorbagy, T. Ichikawa, T. Terasawa, and K. Taguchi. 2006. "3D model application to study residual flow in the Arabian Gulf." *J. Waterway, Port, Coastal, Ocean Eng.* 132 (5): 388–400. [https://doi.org/10.1061/\(ASCE\)0733-950X\(2006\)132:5\(388\)](https://doi.org/10.1061/(ASCE)0733-950X(2006)132:5(388)).
- Baum, M. J., B. Gibbes, A. Grinham, S. Albert, P. Fisher, and D. Gale. 2018. "Near-field observations of an offshore multipoint brine diffuser under various operating conditions." *J. Hydraul. Eng.* 144 (11): 05018007. [https://doi.org/10.1061/\(ASCE\)HY.1943-7900.0001524](https://doi.org/10.1061/(ASCE)HY.1943-7900.0001524).
- Bleninger, T., and G. H. Jirka. 2008. "Modelling and environmentally sound management of brine discharges from desalination plants." *Desalination* 221 (1–3): 585–597. <https://doi.org/10.1016/j.desal.2007.02.059>.
- Blumberg, A. F., Z.-G. Ji, and C. K. Ziegler. 1996. "Modeling outfall plume behavior using far field circulation model." *J. Hydraul. Eng.* 122 (11): 610–616. [https://doi.org/10.1061/\(ASCE\)0733-9429\(1996\)122:11\(610\)](https://doi.org/10.1061/(ASCE)0733-9429(1996)122:11(610)).
- Camacho, R. A., and J. L. Martin. 2013. "Hydrodynamic modeling of first-order transport timescales in the St. Louis Bay Estuary, Mississippi." *J. Environ. Eng.* 139 (3): 317–331. [https://doi.org/10.1061/\(ASCE\)EE.1943-7870.0000647](https://doi.org/10.1061/(ASCE)EE.1943-7870.0000647).
- Chen, C., H. Liu, and R. C. Beardsley. 2003. "An unstructured grid, finite-volume, three-dimensional, primitive equations ocean model: Application to coastal ocean and estuaries." *J. Atmos. Ocean Tech.* 20 (1): 159–186. [https://doi.org/10.1175/1520-0426\(2003\)020<0159:AUGFVT>2.0.CO;2](https://doi.org/10.1175/1520-0426(2003)020<0159:AUGFVT>2.0.CO;2).
- Cucco, A., and G. Umgiesser. 2015. "The Trapping Index: How to integrate the Eulerian and the Lagrangian approach for the computation of the transport time scales of semi-enclosed basins." *Mar. Pollut. Bull.* 98 (1–2): 210–220. <https://doi.org/10.1016/j.marpolbul.2015.06.048>.
- Debler, W., and J. Imberger. 1996. "Flushing criteria in estuarine and laboratory experiments." *J. Hydraul. Eng.* 122 (12): 728–734. [https://doi.org/10.1061/\(ASCE\)0733-9429\(1996\)122:12\(728\)](https://doi.org/10.1061/(ASCE)0733-9429(1996)122:12(728)).
- Devlin, M., et al. 2015. "Changes in the water quality conditions of Kuwait's marine waters: Long term impacts of nutrient enrichment." *Mar. Pollut. Bull.* 100 (2): 607–620. <https://doi.org/10.1016/j.marpolbul.2015.10.022>.
- Dupavillon, J. L., and B. M. Gillanders. 2009. "Impacts of seawater desalination on the giant Australian cuttlefish *Sepia apama* in the upper Spencer Gulf, South Australia." *Mar. Environ. Res.* 67 (4–5): 207–218. <https://doi.org/10.1016/j.marenvres.2009.02.002>.
- Einav, R., and F. Lokiec. 2003. "Environmental aspects of a desalination plant in Ashkelon." *Desalination* 156 (1–3): 79–85. [https://doi.org/10.1016/S0011-9164\(03\)00328-X](https://doi.org/10.1016/S0011-9164(03)00328-X).
- Ghanea, M., M. Moradi, and K. Kabiri. 2016. "A novel method for characterizing harmful algal blooms in the Persian Gulf using MODIS measurements." *Adv. Space Res.* 58 (7): 1348–1361. <https://doi.org/10.1016/j.asr.2016.06.005>.
- Glibert, P. M., et al. 2002. "A fish kill of massive proportion in Kuwait Bay, Arabian Gulf, 2001: The roles of bacterial disease, harmful algae, and eutrophication." *Harmful Algae* 1 (2): 215–231. [https://doi.org/10.1016/S1568-9883\(02\)00013-6](https://doi.org/10.1016/S1568-9883(02)00013-6).
- Global Water Intelligence. 2016. "DesalData: Plants." Accessed July 15, 2016. [www.desaldata.com/projects](http://www.desaldata.com/projects).
- Guo, Q., and G. P. Lordi. 2000. "Method for quantifying freshwater input and flushing time in estuaries." *J. Environ. Eng.* 126 (7): 675–683. [https://doi.org/10.1061/\(ASCE\)0733-9372\(2000\)126:7\(675\)](https://doi.org/10.1061/(ASCE)0733-9372(2000)126:7(675)).
- Hashim, A., and M. Hajjaj. 2005. "Impact of desalination plants fluid effluents on the integrity of seawater, with the Arabian Gulf in perspective." *Desalination* 182 (1–3): 373–393. <https://doi.org/10.1016/j.desal.2005.04.020>.
- Höpner, T., and J. Windelberg. 1997. "Elements of environmental impact studies on coastal desalination plants." *Desalination* 108 (1–3): 11–18. [https://doi.org/10.1016/S0011-9164\(97\)00003-9](https://doi.org/10.1016/S0011-9164(97)00003-9).
- Ibrahim, H. 2017. "Investigation of the impact of desalination on the salinity of the Persian Gulf." Ph.D. thesis, Dept. of Civil and Environmental Engineering, Massachusetts Institute of Technology.
- Im, E.-S., and E. A. B. Eltahir. 2018. "Simulations of the observed 'jump' in the West African monsoon and its underlying dynamics using the MIT regional climate model." *Int. J. Climatol.* 38 (2): 841–852. <https://doi.org/10.1002/joc.5214>.
- Im, E.-S., R. L. Gianotti, and E. A. B. Eltahir. 2014. "Improving the simulation of the West African monsoon using the MIT regional climate model." *J. Clim.* 27 (6): 2209–2229. <https://doi.org/10.1175/JCLI-D-13-00188.1>.
- Jiang, C., Y. Liu, Y. Long, and C. Wu. 2017. "Estimation of residence time and transport trajectory in Tieshangang Bay, China." *Water* 9 (5): 321. <https://doi.org/10.3390/w9050321>.
- Johns, W. E., F. Yao, D. B. Olson, S. A. Josey, J. P. Grist, and D. A. Smeed. 2003. "Observations of seasonal exchange through the Straits of Hormuz and the inferred heat and freshwater budgets of the Persian Gulf." *J. Geophys. Res.* 108 (C12): 21-1–21-18. <https://doi.org/10.1029/2003JC001881>.
- Jong, R. L. D. 1989. "Water resources of GCC: International aspects." *J. Water Resour. Plann. Manage.* 115 (4): 503–510. [https://doi.org/10.1061/\(ASCE\)0733-9496\(1989\)115:4\(503\)](https://doi.org/10.1061/(ASCE)0733-9496(1989)115:4(503)).



- Kim, Y. H., K. Knee, D. Stuebe, and E. Howlett. 2012. "Evaluation of flushing efficiency in an embayment system depending on different channel configurations using FVCOM: A case study in Abu Dhabi." In *Proc., Estuarine and Coastal Modeling*, 118–138. Reston, VA: ASCE.
- Koh, R. C. Y., and N. H. Brooks. 1975. "Fluid mechanics of waste-water disposal in the Ocean." *Annu. Rev. Fluid Mech.* 7 (1): 187–211. <https://doi.org/10.1146/annurev.fl.07.010175.001155>.
- Lattemann, S., and T. Höpner. 2008. "Environmental impact and impact assessment of seawater desalination." *Desalination* 220 (1–3): 1–15. <https://doi.org/10.1016/j.desal.2007.03.009>.
- Locarnini, R. A., A. V. Mishonov, J. I. Antonov, T. P. Boyer, H. E. Garcia, O. K. Baranova, M. M. Zweng, and D. R. Johnson. 2010. *World ocean atlas 2009, volume 1: Temperature*, 184. Edited by S. Levitus. Washington, DC: US Government Printing Office.
- Malfeito, J., J. Díaz-Caneja, M. Fariñas, Y. Fernández-Torquemada, J. M. González-Correa, A. Carratalá-Giménez, and J. Sánchez-Lizaso. 2005. "Brine discharge from the Javea desalination plant." *Desalination* 185 (1–3): 87–94. <https://doi.org/10.1016/j.desal.2005.05.010>.
- Mezhoud, N., M. Temimi, J. Zhao, M. R. A. Shehhi, and H. Ghedira. 2016. "Analysis of the spatio-temporal variability of seawater quality in the southeastern Arabian Gulf." *Mar. Pollut. Bull.* 106 (1–2): 127–138. <https://doi.org/10.1016/j.marpolbul.2016.03.016>.
- Morton, A., I. Callister, and N. Wade. 1997. "Environmental impacts of seawater distillation and reverse osmosis processes." *Desalination* 108 (1–3): 1–10. [https://doi.org/10.1016/S0011-9164\(97\)00002-7](https://doi.org/10.1016/S0011-9164(97)00002-7).
- Nakatsuji, K., and T. Fujiwara. 1997. "Residual baroclinic circulations in semienclosed coastal seas." *J. Hydraul. Eng.* 123 (4): 362–373. [https://doi.org/10.1061/\(ASCE\)0733-9429\(1997\)123:4\(362\)](https://doi.org/10.1061/(ASCE)0733-9429(1997)123:4(362)).
- Ng, K. Y., S. Eftekharzadeh, and P. J. Ryan. 2001. "Multi-dimensional hydrodynamic and transport modeling of seawater intake and discharge in a shallow coastal environment." In *Proc., Bridging the Gap*, 1–10. Reston, VA: ASCE.
- Palomar, P., and I. Losada. 2010. "Desalination in Spain: Recent developments and recommendations." *Desalination* 255 (1–3): 97–106. <https://doi.org/10.1016/j.desal.2010.01.008>.
- Pérez-Díaz, B., S. Castanedo, P. Palomar, F. Henno, and M. Wood. 2019. "Modeling nonconfined density currents using 3D hydrodynamic models." *J. Hydraul. Eng.* 145 (3): 04018088. [https://doi.org/10.1061/\(ASCE\)HY.1943-7900.0001563](https://doi.org/10.1061/(ASCE)HY.1943-7900.0001563).
- Purnalna, A., H. Al-Barwani, and M. Al-Lawatia. 2003. "Modeling dispersion of brine waste discharges from a coastal desalination plant." *Desalination* 155 (1): 41–47. [https://doi.org/10.1016/S0011-9164\(03\)00237-6](https://doi.org/10.1016/S0011-9164(03)00237-6).
- Rego, J. L., C. Li, and I. Hossain. 2010. "The flushing of Louisiana's Coastal Bays under Hurricane conditions." In *Proc., Estuarine and Coastal Modeling*, 89–107. Reston, VA: ASCE.
- Reynolds, R. M. 1993. "Physical oceanography of the Gulf, Strait of Hormuz, and the Gulf of Oman—Results from the Mt Mitchell expedition." *Mar. Pollut. Bull.* 27: 35–59. [https://doi.org/10.1016/0025-326X\(93\)90007-7](https://doi.org/10.1016/0025-326X(93)90007-7).
- Reynolds, R. W., T. M. Smith, C. Liu, D. B. Chelton, K. S. Casey, and M. G. Schlax. 2007. "Daily high-resolution-blended analyses for sea surface temperature." *J. Clim.* 20 (22): 5473–5496. <https://doi.org/10.1175/2007JCLI1824.1>.
- Roberts, D. A., E. L. Johnston, and N. A. Knott. 2010. "Impacts of desalination plant discharges on the marine environment: A critical review of published studies." *Water Res.* 44 (18): 5117–5128. <https://doi.org/10.1016/j.watres.2010.04.036>.
- Roberts, P. J. W. 1999. "Modeling Mamala bay outfall plumes. II: Far Field." *J. Hydraul. Eng.* 125 (6): 574–583. [https://doi.org/10.1061/\(ASCE\)0733-9429\(1999\)125:6\(574\)](https://doi.org/10.1061/(ASCE)0733-9429(1999)125:6(574)).
- Roberts, P. J. W., C. D. Hunt, M. J. Mickelson, and X. Tian. 2011. "Field and model studies of the Boston Outfall." *J. Hydraul. Eng.* 137 (11): 1415–1425. [https://doi.org/10.1061/\(ASCE\)HY.1943-7900.0000445](https://doi.org/10.1061/(ASCE)HY.1943-7900.0000445).
- Sadrinasab, M., and J. Kämpf. 2004. "Three-dimensional flushing times of the Persian Gulf." *Geophys. Res. Lett.* 31 (L24301): 1–4. <https://doi.org/10.1029/2004GL020425>.
- Sale, P. F., et al. 2011. "The growing need for sustainable ecological management of marine communities of the Persian Gulf." *Ambio* 40 (1): 4–17. <https://doi.org/10.1007/s13280-010-0092-6>.
- Saleh, D. K. 2010. "Stream gage descriptions and streamflow statistics for sites in the Tigris River and Euphrates River Basins, Iraq." In Vol. 540 of *Data series*, 146. Washington, DC: USGS.
- Shahvari, A., and J. Yoon. 2014. "Brine discharge load design and optimization framework for desalination process using mixing plume criteria and discharge pipe length augmentation." In *Proc., World Environmental and Water Resources Congress*, 666–678. Reston, VA: ASCE.
- Shehhi, M. R. A., I. Gherboudj, and H. Ghedira. 2014. "An overview of historical harmful algae blooms outbreaks in the Arabian Seas." *Mar. Pollut. Bull.* 86 (1–2): 314–324. <https://doi.org/10.1016/j.marpolbul.2014.06.048>.
- Sugden, W. 1963. "The hydrology of the Persian Gulf and its significance in respect to evaporite deposition." *Am. J. Sci.* 261 (8): 741–755. <https://doi.org/10.2475/ajs.261.8.741>.
- Thoppil, P. G., and P. J. Hogan. 2010. "A modeling study of circulation and eddies in the Persian Gulf." *J. Phys. Oceanogr.* 40 (9): 2122–2134. <https://doi.org/10.1175/2010JPO4227.1>.
- Thu, K., Y.-D. Kim, G. Amy, W. G. Chun, and K. C. Ng. 2014. "A synergetic hybridization of adsorption cycle with the multi-effect distillation (MED)." *Appl. Therm. Eng.* 62 (1): 245–255. <https://doi.org/10.1016/j.applthermaleng.2013.09.023>.
- Tsiourtis, N. X. 2008. "Criteria and procedure for selecting a site for a desalination plant." *Desalination* 221 (1–3): 114–125. <https://doi.org/10.1016/j.desal.2007.01.073>.
- Voutchkov, N. 2018. "Energy use for membrane seawater desalination—Current status and trends." *Desalination* 431 (Apr): 2–14. <https://doi.org/10.1016/j.desal.2017.10.033>.
- Xue, P., and E. A. B. Eltahir. 2015. "Estimation of the heat and water budgets of the Persian (Arabian) Gulf using a regional climate model." *J. Clim.* 28 (13): 5041–5062. <https://doi.org/10.1175/JCLI-D-14-00189.1>.
- Zhang, J., Y. Guo, Y. Shen, and L. Zhang. 2008. "Numerical simulation of flushing of trapped salt water from a bar-blocked estuary." *J. Hydraul. Eng.* 134 (11): 1671–1676. [https://doi.org/10.1061/\(ASCE\)0733-9429\(2008\)134:11\(1671\)](https://doi.org/10.1061/(ASCE)0733-9429(2008)134:11(1671)).
- Zhao, J., and H. Ghedira. 2014. "Monitoring red tide with satellite imagery and numerical models: A case study in the Arabian Gulf." *Mar. Pollut. Bull.* 79 (1–2): 305–313. <https://doi.org/10.1016/j.marpolbul.2013.10.057>.